Direct Sulfation of Limestone

Guilin Hu, Kim Dam-Johansen, and Stig Wedel
CHEC, Dept. of Chemical Engineering, Technical University of Denmark, 2800 Lyngby, Denmark

Jens Peter Hansen
FLSmidth A/S, Denmark

DOI 10.1002/aic.11129

The direct sulfation of limestone was studied in a laboratory fixed-bed reactor. It is found that the direct sulfation of limestone involves nucleation and crystal grain growth of the solid product (anhydrite). At 823 K and at low-conversions (less than about 0.5 %), the influences of SO_2, O_2 and CO_2 on the direct sulfation of limestone corresponds to apparent reaction orders of about 0.2, 0.2 and −0.5, respectively. Water is observed to promote the sulfation reaction and increase the apparent reaction orders of SO_2 and O_2. The influence of O_2 at high O_2 concentrations (> about 15 %) becomes negligible. In the temperature interval from 723 K to 973 K, an apparent activation energy of about 104 kJ/mol is observed for the direct sulfation of limestone. At low temperatures and low conversions, the sulfation process is most likely under mixed control by chemical reaction and solid-state diffusion. The nucleation and crystal grain growth of the solid product, and this mixed control mechanism provide satisfactory explanations of the various phenomena related to the direct sulfation of limestone, such as porosity in the product layer, the variation of the apparent reaction orders of SO_2, O_2 and CO_2 with reaction conditions and the influence of water. © 2007 American Institute of Chemical Engineers *AIChE J,* 53: 948–960, 2007

Keywords: kinetics, sulfation, mechanism, limestone, sulfur dioxide, desulfurization, nucleation

Introduction

The direct sulfation of limestone is defined as the sulfation reaction between SO_2 and limestone in the uncalcined state, and can be expressed by the following overall reaction

$$CaCO_3(s) + SO_2(g) + 0.5O_2(g) \rightarrow CaSO_4(s) + CO_2(g) \quad (1)$$

The direct sulfation reaction is, for example, practically relevant for desulfurization by direct dry sorbent injection during pressurized fluid-bed combustion (PFBC), and SO_2 absorption on limestone in the cyclone preheater that is used in cement production. Cement is currently produced mainly by the so-called "dry-process". In this production process, a multistage cyclone preheater is used for preheating of the raw meal—a powder mixture of the raw materials—by direct countercurrent heat exchange with the hot flue gas from the calciner for raw meal calcination, and the rotary kiln for clinker burning in the downstream of the production process. During the heating process, the sulfation reaction between limestone particles—the major constituent in the raw meal—and SO_2 that is formed mainly by the oxidation of pyrite contained in the raw meal takes place. The CO_2 partial pressure in the hot flue gas is normally around 30 vol. %, which is sufficiently high to prevent the calcination of limestone at the highest temperature approximately 1073 K in the cyclone preheater. The sulfation reaction in the cyclone preheater, is, thus, the direct sulfation reaction.

In previous decades, the direct sulfation of limestone has been studied extensively mainly because of the potential of

---

Correspondence concerning this article should be addressed to G. Hu at gh@kt.dtu.dk.

direct dry sorbent injection as a simple and economical desulfurization method during PFBC. Hu et al.[1] recently performed a comprehensive review of the literature concerning this reaction. The review highlights that a number of phenomena observed concerning this reaction by different authors are either not explained satisfactorily or not explained at all. The following are some examples:

- The product layer formed by the direct sulfation of limestone is porous,[2,3,4] despite the fact that the molar volume of the formed solid product ($CaSO_4$) is much larger than that of calcite. The porosity and pore size increase with increasing temperature and decrease with increasing conversion of the limestone.
- The influences of the gaseous reactants and product (SO_2, O_2 and CO_2) on the direct sulfation of limestone were observed to vary with reaction conditions. The apparent reaction orders of SO_2 observed by various authors[5,6,7,8] are significantly lower than unity, while the apparent reaction order of O_2 was observed to drop to zero at high O_2 concentrations.[4,9,10] Higher CO_2 concentrations were observed to depress the direct sulfation reaction under certain reaction conditions.[11,12,13]
- The effective diffusivity in the product layer was observed to decrease with increasing conversion and SO_2 concentration.[3,7,8,10]
- Water can both significantly promote the direct sulfation reaction and increase the apparent reaction order of SO_2[3,5] although water is not considered to participate in the reaction as a reactant.

Furthermore, previous kinetic studies are also heavily empirical, which seriously limits the applicability of kinetic data published in the literature. One of the main reasons for the difficulty in explaining the earlier observations, and for the heavily empirical methods applied in previous kinetic studies is the limited understanding of the mechanism of the direct sulfation of limestone.

The study described in this article is part of a project that aims at a better understanding of the sulfation reaction taking place in the cyclone preheater used in cement production with the final purpose of reducing SO_2 emissions from the production process. In the following, the main experimental results of this study are presented. A new mechanism for the direct sulfation of limestone is proposed based on the experimental results. The various phenomena of the direct sulfation of limestone that are observed in this and earlier studies are discussed and explained in terms of the obtained results and the new mechanism.

Experimental

Reactor setup

All experiments were performed in a quartz fixed-bed reactor as illustrated in Figure 1. The reactor was originally developed by Dam-Johansen et al.[14–17] for studying the sulfation reaction between SO_2 and limestone. The reactor consists of a quartz shell and a removable inner tube that contains the sample bed; the inner diameter of the inner tube is 16 mm. The reactor is electrically heated by three separate heating sections. Each of the heating sections has its own temperature controlling system. The reaction temperature is measured by a thermocouple located immediately beneath the sample bed. Temperature mapping of the reactor showed that the temperature variation was less than 2 degrees between the measuring point, and the point that is about 10 cm over the bed. It was observed during each experiment that the temperature increased no more than about 0.5–1 degree after SO_2 was introduced. The isothermal reaction condition is therefore considered to be fulfilled.

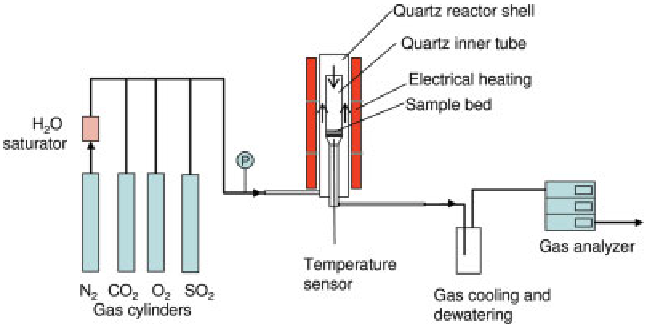

Figure 1. Sulfation reactor setup.

[Color figure can be viewed in the online issue, which is available at www.interscience.wiley.com.]

The required gases (SO_2, O_2, CO_2 and N_2) are supplied from gas cylinders, with the flow of each gas controlled by a mass flow controller. Water vapor is added to the gas mixture by passing the CO_2 or N_2 gas through liquid water in a heated container. The container is specially designed to secure saturation of the passing gas. The gas mixture enters the reactor at the bottom and is preheated to the required temperature before it reaches the sample bed. Following the reaction, the gas mixture flows out of the bottom of the reactor and is cooled to approximately 278 K to remove water from the gas. The gas is then analyzed for SO_2, O_2, and CO_2 by on-line gas analyzers. The concentrations of SO_2, O_2, and CO_2, temperature and pressure upstream of the bed are continuously measured and logged via a data acquisition system.

Samples

Three types of limestone were used for the experiments: a soft and porous bryozoan limestone from Faxe Kalk in Denmark (referred to hereafter as Faxe Bryozo), a hard and dense limestone from Obajana, Nigeria, provided by FLSmidth A/S in Denmark (referred to hereafter as Obajana Limestone), and Iceland Spar (a naturally occurring and very pure crystalline calcite) provided by the Geological Museum, Denmark. Faxe Bryozo was in powder form when purchased. The structure of this type of limestone has been thoroughly studied by Dam-Johansen et al.[14–17] in relation to their extensive study of sulfation of various limestones. Particles of Faxe Bryozo are agglomerates of primary particles of a few micrometers in size. The three limestones were ground and sieved. Table 1 shows the properties of these limestones and the particle sizes used for the experiments.

The limestone particles prepared for the experiments were dried in an oven at 393 K for about 12 h, and then stored in airtight containers. For each experiment, a sample weight of 0.25–2.8 g was used depending on the reaction temperatures. Large sample weights were used for experiments at lower-temperatures and small sample weights for experiments at higher-tem-

Table 1. Properties of the Limestones Used for the Experiments

Limestone	Faxe Bryozo	Obajana Limestone	Iceland Spar
Composition*:			
$CaCO_3$ (w %)	97	94	>99.5
Elemental analysis (w %):			
Na	<detection limit of 0.001	0.026	<detection limit of 0.001%
Mg	0.26	0.64	0.005
Al	0.026	0.31	<detection limit of 0.001%
Si	0.23	1.2	<detection limit of 0.001%
P	0.014	0.005	<detection limit of 0.001%
S	0.03	0.03	0.04
K	0.0054	0.15	<detection limit of 0.001%
Ca	39	38	40
Ti	0.002	0.019	<detection limit of 0.001%
V	0.002	0.002	<detection limit of 0.001%
Cr	<detection limit of 0.001	0.001	<detection limit of 0.001%
Mn	0.02	0.004	0.006
Fe	0.047	0.19	0.02
Zn	0.0014	< detection limit of 0.001	<detection limit of 0.001%
Sr	0.042	0.27	0.02
Particle size (mm)	0.18–0.25	0.2–0.3	0.18–0.25
Total surface area** (m^2/g)	0.78	0.19	NA

*Determined by Wavelength Dispersive X-Ray (Philips PW2400).
**Determined by BET (Micrometrics ASAP 2000).

peratures to obtain a concentration drop of SO_2 around 10% at higher SO_2 concentrations (> about 1,000 ppm) and 10–30% at lower SO_2 concentrations (< about 500 ppm), which corresponds to a SO_2 concentration drop of about 20–200 ppm. The uncertainty of SO_2 measurement by the online gas analyzer is less than ± 2.5 ppm at high SO_2 concentrations (>500 ppm), and less than ± 0.5 ppm at low SO_2 concentrations (<500 ppm). The concentration-drop range encountered during the experiments ensures reliable measurements, and nearly differential reaction conditions in the reactor. It was verified that the variation in sample weight had no noticeable influence on the sulfation rate under the reaction conditions used.

Experimental procedure

For each run, the reactor was preheated to the required temperature. Gas flow through the sample bed was maintained at 1 l/min (298 K, atmospheric pressure). Calculations show that gas film resistance was negligible under these conditions. Experiments conducted using samples of different particle sizes also demonstrated that intraparticle diffusion resistance was insignificant under the applied reaction conditions. The gases were mixed to the required composition, which was verified by the gas analyzers. The inner tube was taken out, and a weighed sample of limestone particles was poured into the bed. The surface of the sample bed was leveled by gently knocking the tube. The tube with the sample was then put back in the reactor and was heated again. All the gases except SO_2 were mixed and admitted into the reactor. The heating-up generally took 5–8 min. After the temperature reached the set point, SO_2 gas was added to the gas stream. The reaction then started, and continued for a period from 5 min to a couple of hours depending on the purposes.

Experimental conditions

In this investigation the following parameters were used: temperature: 723–973 K; SO_2 concentration: 50–1,800 ppm (vol.); O_2 concentration: 0.5–45 (vol.) %; CO_2 concentration: 5–52 (vol.) %; H_2O concentration: 0–7.5 (vol.) %. These conditions cover typical temperatures and gas compositions in the cyclone preheater used in cement production.

Results

Data treatment

For the calculation of conversion rate and conversion of the limestone sample, the following equations are used.

Conversion rate at any time

$$dx/dt = (PV(y_{SO_2,in} - y_{SO_2,out})/(RT))/(W\zeta/M_{CaCO_3}) \quad (s^{-1}) \tag{2}$$

Increase in conversion during the time interval of sampling (Δt) at any time:

$$\Delta x_t = [(PV(y_{SO_2,in} - y_{SO_2,out})/(RT))/(W\zeta/M_{CaCO_3})]\Delta t \tag{3}$$

Conversion at time t is obtained by summing Δx.

Deconvolution[18] of the measured data by Fourier transform showed that in the first half minute of the reaction the SO_2 concentration measured by the online gas analyzer deviated significantly from the true SO_2 concentration immediately after the sample bed, because of the influence of residence-time distribution (RTD) in the system. After this short period, the influence of RTD was negligible due to the relatively slow change with time in SO_2 concentration after the bed. Figure 2 illustrates such variations of the outlet SO_2 concentration.

To avoid uncertainties caused by the RTD in the initial period, only data for the period from 180–480 s are used. Due to the closely linear increase of conversion with reaction time in this period, the average conversion rate calculated by the following equation is used for evaluations of other kinetic parameters

$$(dx/dt)_{av} = \Delta x/\Delta t = (x_{480s} - x_{180s})/300 \ (s^{-1}). \tag{4}$$

The vertical bar "I" in all the figures represents the maximum uncertainty estimated via the method of error propaga-

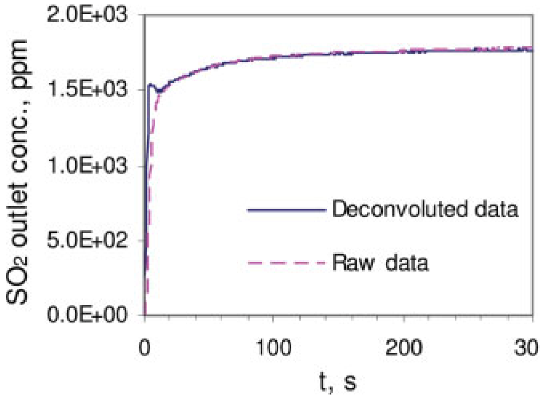

Figure 2. Influence of RTD to outlet SO_2 concentrations (reaction conditions: limestone: Faxe Bryozo; T: 823 K, P: 0.11 MPa; SO_2 (inlet): 1830 ppm SO_2; O_2: 3%; CO_2: 30%).

[Color figure can be viewed in the online issue, which is available at www.interscience.wiley.com.]

tion. In the following sections, the main results are introduced. Some additional results are introduced in the discussion section.

Influence of gases

To assess the significance of the influence of each gas at different concentrations, sulfation experiments were carried out by varying the concentration of the concerned gas while keeping the concentrations of other gases constant. The investigated gases include SO_2, O_2, CO_2, and H_2O. The following are the main results.

SO_2. The influence of SO_2 concentration on the conversion rate of Faxe Bryozo was investigated at two oxygen concentrations and is shown in Figure 3. The increase in the average conversion rate with SO_2 concentration is relatively weak, and corresponds to an average apparent reaction order of 0.22 at 3% oxygen, and 0.17 at 0.5% oxygen, which are much lower than the values of 0.76 observed by Yang et al.,[5] 0.49 by Iisa et al.,[6] 0.4 by Krishnan[7] and 0.58 by Qiu et al.[8] The relatively low apparent reaction order of SO_2 may be related to the much lower-temperatures used in this study than in the earlier studies. The influence of SO_2 on the direct sulfation reaction seems to be affected by the presence of water in the gas, as an addition of 7.5% water in the gas increased the average apparent reaction order of SO_2 to approximately 0.4 in the SO_2 concentration interval from 500 to 1,800 ppm. This phenomenon is principally in agreement with the observation by Yang et al.[5]

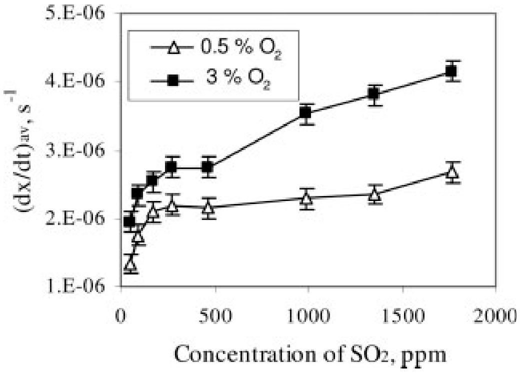

Figure 3. Variation of the average conversion rate of Faxe Bryozo with SO_2 concentrations at 823 K (other conditions: P: 0.11 MPa; CO_2: 30%; H_2O: 0%).

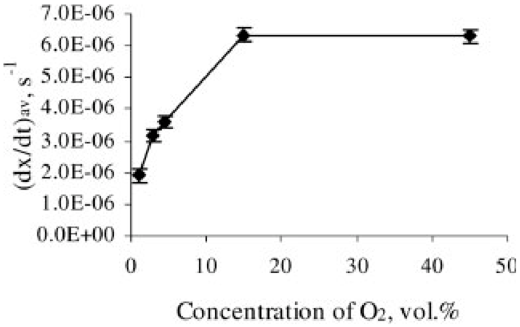

Figure 4. Variation of the average conversion rate of Faxe Bryozo with O_2 concentrations at 823 K (other conditions: P: 0.11 MPa; SO_2: 1800 ppm; CO_2: 30%; H_2O: 7.5%).

O_2. The influence of O_2 concentration on the conversion rate of Faxe Bryozo in the presence of 7.5% water in the gas is shown in Figure 4. The conversion rate increases with increasing O_2 concentration at O_2 concentrations up to approximately 15%. The influence of O_2 up to this concentration corresponds to an apparent reaction order of around 0.4. At higher O_2 concentrations the conversion rate did not increase further, giving an apparent reaction order of zero. This phenomenon is principally in agreement with observations by Iisa et al.,[9] Alvarez et al.[10] and Liu et al.[4] The presence of water seems to create a higher-reaction order for O_2 as for SO_2, as the average reaction order at low O_2 concentrations, and without water addition (evaluated by using data presented in Figure 3) is only about 0.2.

CO_2. The influence of CO_2 concentration on the conversion rate of Faxe Bryozo is shown in Figure 5. The conversion rate decreases consistently with increasing CO_2 concentration. The influence of CO_2 concentration on the conversion rate corresponds to an apparent reaction order of approximately –0.5. The observed negative influence of CO_2 on the direct sulfation of limestone is in agreement with pre-

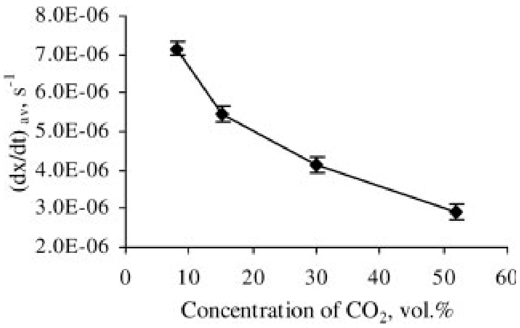

Figure 5. Variation of the average conversion rate of Faxe Bryozo with CO_2 concentrations at 823 K. (other conditions: P: 0.11 MPa; SO_2: 1,800 ppm; O_2: 3%; H_2O: 0%).

vious observations by Ulerrich et al.,[11] Dam-Johansen,[12] and Tullin et al.[13]

H_2O. H_2O has no doubt a promoting effect on the direct sulfation of limestone. Figure 6 shows the conversion rate vs. time curve at 923 K with and without water in the gas. Initially water was not added to the gas. The figure shows a decreasing conversion rate with the reaction time. At the reaction time of about 600 s, water was added to the gas at a concentration of about 7.5 %. The addition of water resulted in an abrupt increase in the conversion rate. The conversion rate continued to decrease with the reaction time at almost the same rate as before the addition of water. At the reaction time of about 950 s, the addition of water was ceased; this caused an abrupt drop in the conversion rate. A similar experiment performed at 823 K yielded similar results. The promoting effect of water on the direct sulfation of Faxe Bryozo is in agreement with the observation by Hajaligol et al.[3] The presence of water seems to cause changes in the sulfation behavior of the limestone, which is reflected by the almost constant-conversion rate after the stop of water addition.

Influence of temperature

To assess the influence of temperature on the sulfation reaction, the apparent activation energy is evaluated in the temperature interval from 723 K to 973 K for both Faxe Bryozo and Obajana Limestone. The conversion rates at different temperatures were measured at the same inlet gas concentrations (vol. %). Due to the differential reaction conditions in the reactor, the low-reaction orders of SO_2 and O_2 and the negative reaction order of CO_2, the contributions from the small variations of the gas concentrations caused by the different temperatures to the conversion rates were estimated to be insignificant. The activation energies are thus directly evaluated by plotting $\ln((dx/dt)_{av})$ againt 1/T.

As shown in Figure 7, the apparent activation energy is evaluated to be 104 kJ/mol for Faxe Bryozo and 103 kJ/mol for Obajana Limestone. These two values are essentially equal despite the very different morphologies of these two limestones. The values are also quite close to those obtained by Fuertes et al.[19] (96 kJ/mol), Krishnan et al.[7] (110–138 kJ/mol) and Qiu et al.[8] (96.8 kJ/mol) at low conversions.

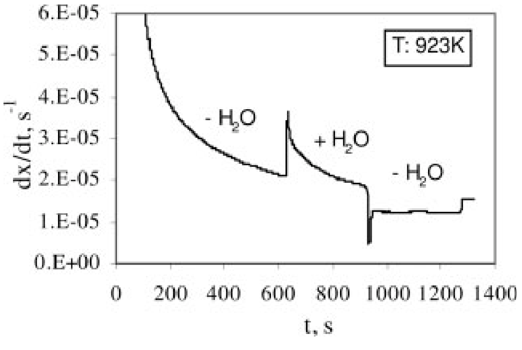

Figure 6. Influence of water addition on the conversion rate of Faxe Bryozo at 923 K (other conditions: P: 0.11 MPa; SO_2: 1,800 ppm; O_2: 3%; CO_2: 30%; H_2O: 0–7.5%).

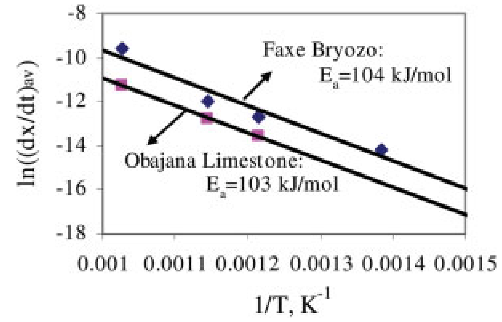

Figure 7. Variation of the average conversion rate with reaction temperature (other conditions: P: 0.11 MPa; SO_2: 1,800 ppm; O_2: 3%; CO_2: 30%; H_2O: 7.5%).

[Color figure can be viewed in the online issue, which is available at www.interscience.wiley.com.]

Sulfation product

The Faxe Bryozo particles sulfated at 873 and 973 were analyzed by X-ray powder diffraction. Anhydrite ($CaSO_4$) was the only identified solid product. The formation of anhydrite is in good agreement with the findings by Murthy et al.,[20] Ljungström and Lindqvist,[21] Dam-Johansen et al.,[16] and Tullin et al.[13]

Morphological change of the sulfated limestone particles

The surface morphologies of the limestone particles before and after the sulfation were examined by SEM (scanning electron microscope). The SEM examinations revealed that the direct sulfation of limestone involves nucleation and crystal grain growth of the solid product (anhydrite), which is well demonstrated in Figures 8–10.

Figure 8 shows SEM images of particle surfaces of Faxe Bryozo before and after the sulfation reaction at 823–973 K. Figure 8b shows the sulfated particle surfaces, which apparently become slightly smoothened and rounded compared to the unreacted particles (Figure 8a). Individual crystal grains of the solid product are not visible. However, powder patterns of X-ray diffraction of the same sample used for Figure 8b indicates the existence of anhydrite crystals, as the powder patterns showed actually the characteristic strong peak at $2\theta = 25.5^\circ$ for anhydrite (other peaks are too weak to be seen). The magnification of the SEM images is most likely insufficient in this case to show the very small crystal grains. At 873 K, the formation of product crystal grains is already visible (Figure 8c) after 10 min sulfation. At 973 K, the particle surfaces are covered byproduct crystal grains after 10 min sulfation (Figure 8d).

Figures 9 and 10 show particle surfaces of Obajana Limestone and Iceland Spar, respectively, before and after sulfation at 973 K. The formation of crystal grains of the solid product is clearly visible.

Both the powder patterns of X-ray diffraction of the sulfated samples and sulfur mapping of the sulfated Iceland Spar particle by Energy-Dispersive X-ray Analysis (EDXA) supported that the crystal grains formed by the sulfation reaction are crystal grains of anhydrite.

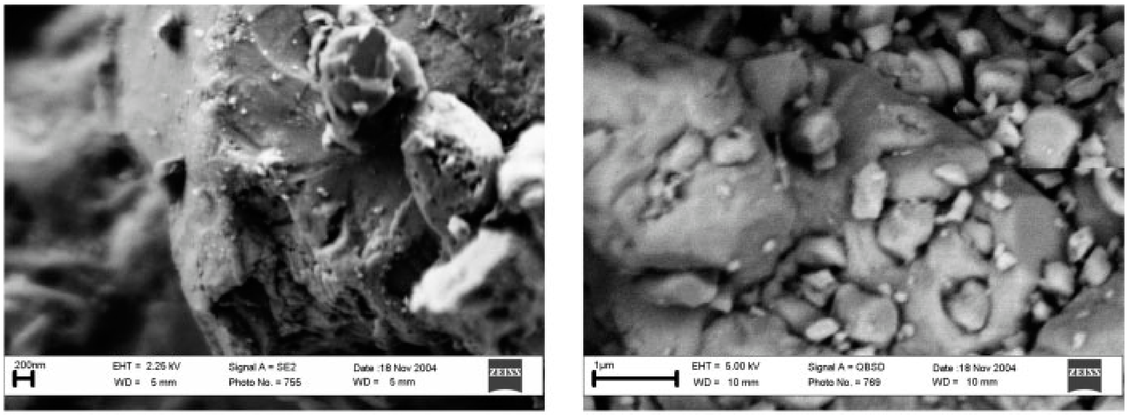

a. Unreacted Faxe Bryozo

b. Faxe Brozo sulfated at 823 K for 90 min. ($x \approx 1$ %)

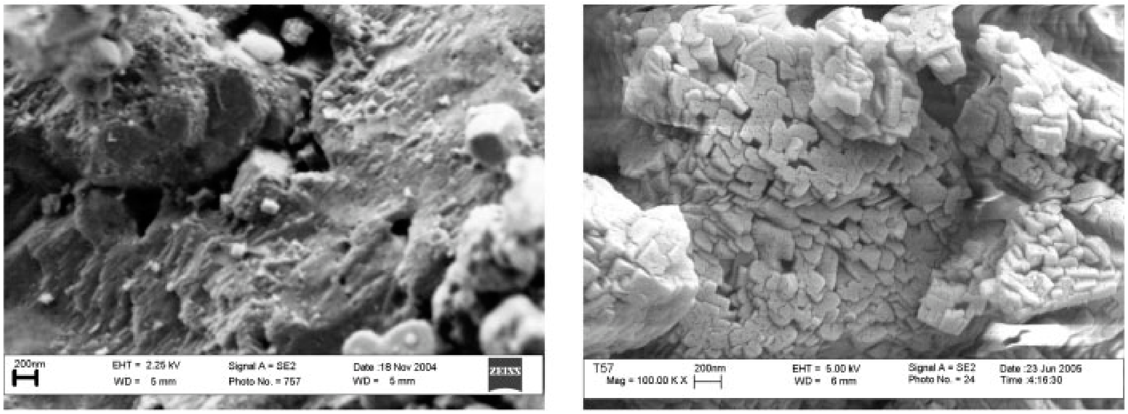

c. Faxe Bryozo sulfated at 873 K for 10 min. ($x \approx 0.5$ %)

d. Faxe Bryozo sulfated at 973 K for 10 min. ($x \approx 4.5$ %)

Figure 8. SEM images of Faxe Bryozo particles before and after sulfation at 823–973 K (other conditions: P: 0.11 MPa; SO_2: 1,800 ppm; O_2: 3%; CO_2: 30%; H_2O: 0%).

The above SEM images demonstrate that the formation of the product crystal grains is oriented[22]—the product crystal grain is directly connected to calcite in lattice level and grows in a definite direction which is determined by the direction of the lattice surface on which the nucleation and growth take place. This phenomenon is discussed further in the following section.

Discussions

The experimental results allow us to propose a mechanism for the direct sulfation of limestone and give a qualitative assessment of its validity. Various subjects concerning the direct sulfation of limestone are discussed, including phenomena observed in this and earlier studies, such as porosity in the product layer, variation in the apparent reaction orders of SO_2, O_2, and CO_2, the controlling mechanism and the influence of water. Some simple modeling considerations are also included.

Mechanism of the direct sulfation of limestone

Sulfation Process. As shown earlier, the direct sulfation of limestone involves nucleation and crystal grain growth of the solid product (anhydrite). The occurrence of nucleation means that the sulfation of the limestone may be divided into two stages. The first stage extends from the start of the sulfation reaction to the initiation of nucleation of the formed solid product since the nucleation process requires the sulfate concentration at the surface to reach a critical level for the formation of stable nuclei. The second stage involves further sulfation and the growth of the formed nuclei. It can be imagined that a thin layer may exist at the surface of the unreacted core that acts as a kind of parent layer for both nucleation and subsequent growth. There is no direct evidence that can give a clear indication on the chemical properties of this parent layer. One possibility is that this thin layer is a solid solution of the formed product anions in the parent structure of calcite. The surface of the parent layer is the gas-solid reactant interface, as well as the reaction front for the sulfation reaction. Formed sulfate ions (SO_4^{2-}) diffuse in solid state through the parent layer to the root of the product crystal grains and feed the growth process. This process is illustrated schematically in Figure 11.

In addition to the commonly known steps, such as gas film diffusion, pore diffusion in the particle and product layer, and chemical reaction,[18,23] the sulfation of limestone, thus, involves two extra steps: solid-state diffusion and the nuclea-

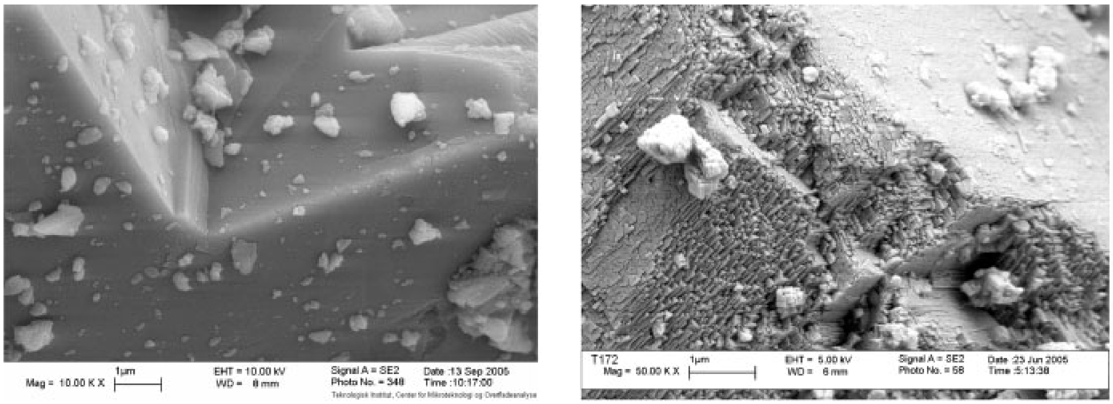

a. Unreacted Obajana Limestone

b. Obajana Limestone sulfated at 973K for 60 min. ($x \approx 5$ %)

Figure 9. SEM images of Obajana Limestone particles before and after sulfation at 973 K (other conditions: P: 0.11 MPa; SO_2: 1,800 ppm; O_2: 3%; CO_2: 30%; H_2O: 0%).

tion-growth process. The sequence of these steps is illustrated in Figure 12.

With the progress of the sulfation, the unreacted core shrinks. The free surface area of the parent layer—the surface area of the parent layer that is directly available for the sulfation reaction—decreases because of both the shrinkage of the unreacted core and the shielding effect of the formed nuclei/crystal grains of the solid product.

Solid-state diffusion and the nucleation-growth process

As described earlier, the sulfation process involves oriented nucleation and crystal grain growth of the solid product. Oriented nucleation usually takes place when the nuclei of the new phase and the substrate have a close two-dimensional (2-D) or 3-D match in their crystal-lattice structures (usually termed epitaxy and topotaxy, respectively).[22] This oriented nucleation and growth is particularly clear with Iceland Spar. Iceland Spar is a natural and pure calcite crystal in relatively large sizes. The SEM image of ground particles (Figure. 10a) shows clearly fractures and the smooth cleavages. The formation of crystal grains of the solid product takes place only at fractures that are perpendicular to the cleavages and with same orientation (Figure 10(b–c)). The situation is similar with Obajana Limestone. Faxe Bryozo consists of small and randomly orientated calcite grains; this is the reason for the apparently random orientation of the product crystal grains. The special preferred orientation of the product crystal grains indicates that they are directly rooted on the crystal lattice of calcite. That is, the crystal lattices of the product crystal grains and the substrate (calcite) are directly connected. The preference of particular sides for the nucleation is due to crystallographic reasons: the nucleation of the solid product prefers the sides/faces of the substrate (calcite) that have similar lattice structure, such as the distance between the cations (Ca^2) and crystallographic angles. Examination of the crystal lattice structures of calcite and anhydrite reveals a very close 2-D lattice match (epitaxy) (distance between cations (Ca^2) and angles) between, for example, the lattice plane (-1,1,0) of anhydrite and the lattice plane (1,0,4) of calcite. Details about this lattice match are discussed in a separate article. The growth is upward, most probably also determined by the fact that the lattice match between the nuclei and the substrate is 2-D.

The oriented nucleation also implies that the parent layer has not lost the basic lattice structure of calcite; this supports the assumption of the formation of a solid solution of the formed product ions in the crystal lattice structure of calcite. Except for the surface of the parent layer where the concentration of the product ions may be quite high, the fraction of product ions in the crystal lattice of calcite in the parent layer is expected to be relatively low; otherwise the crystal lattice structure of calcite may become unstable.

Figures 8–10 show that the product crystal grains grow up from the substrate, just like bamboo shoots. For nucleation and subsequent growth, the product ions must diffuse to the nucleation/growth sites. The diffusion process possibly takes place in the way illustrated in Figure 13.

The diffusion proceeds by point defects,[22] which are most likely vacancies of cations and anions in the crystal lattice of both the product and the substrate (calcite). As illustrated in Figures 11 and 13, sulfate is first formed at the surface of the parent layer. The sulfate ions then diffuse to the root of the grain, and fill the available vacancies in the root. The continuous supply of sulfate ions formed by the sulfation reaction at the surface of the parent layer to the root provides a driving force for the formation of a new layer of the crystal at the outer surface of the crystal grain because the ions that jump out of the lattice sites to the surface of the grain (the jumping-out of the lattice ions to the surface is a coupled process with the formation of point defects) are less likely to jump back due to the continuous filling-up of vacancies at the root. It is possible that movement of the ions partly may proceed synchronized. The movement of cations (Ca^2) is considered to take place in the same way as that for sulfate ions. During this process, carbonate ions have to diffuse to the surface of the parent layer to facilitate the continuation of the sulfation reaction.

With the growth of the grains, the diffusion resistance increases because of the greater diffusion distance. This may be the reason for the rather uniform grain size as shown in Figures 8–10. The grains may at last detach from the substrate (calcite) because of various stresses, allowing new

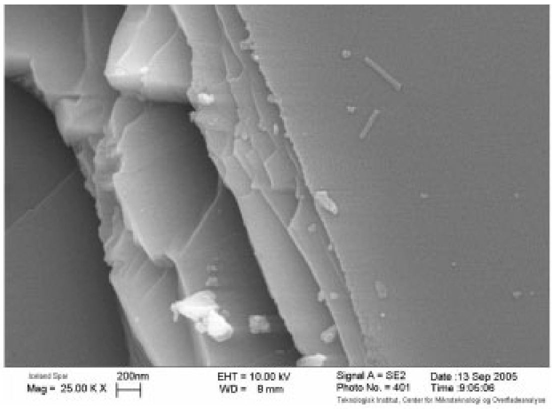

a. Unreacted Iceland Spar

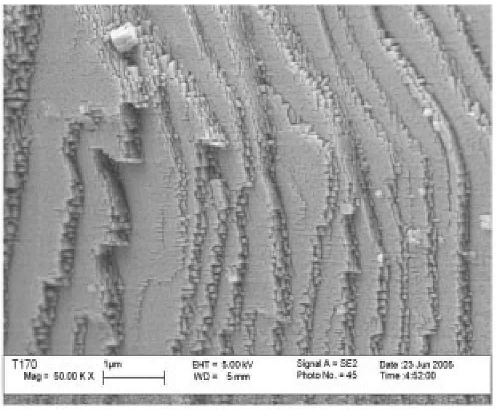

b. Iceland Spar sulfated at 973K for 30 min. ($x \approx 2.7$ %)

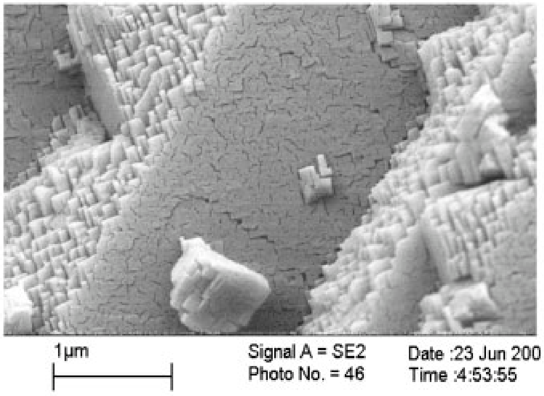

c. Iceland Spar sulfated at 973K for 30 min. ($x \approx 2.7$ %)

Figure 10. SEM images of Iceland Spar particles before and after sulfation at 973 K (other conditions: P: 0.11 MPa; SO_2: 1800 ppm; O_2: 3%; CO_2: 30%; H_2O: 0%).

nuclei to form at places where the sulfate concentration reaches the critical level. The formed product layer is a collection of crystal grains of the solid product.

Chemical reaction at the gas-solid reactant interface

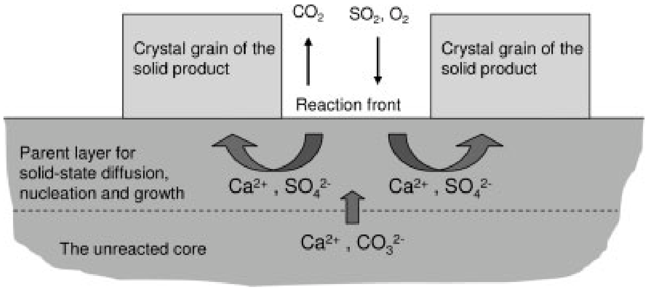

Figure 11. Sulfation process.

In the mechanism described earlier, the chemical reaction is assumed to take place mainly at the free surface of the parent layer. Based on experimental observations and some theoretical considerations, the chemical reaction is suggested to proceed by the following multistep mechanism:

Step 1: adsorption of SO_2 in active sites at the surface of the parent layer

$$SO_2(g) + [\ ]_v(s) \underset{k_{12}}{\overset{k_{11}}{\rightleftarrows}} [SO_2]_v(s) \tag{5}$$

Step 2: conversion of the adsorbed SO_2 to sulfite ions

$$[SO_2]_v(s) + CO_3^{2-}(s) \xrightarrow{k_{21}} \left[SO_3^{2-}\right](s) + [CO_2]_v(s) \tag{6}$$

Step 3: formation of oxygen radicals in gas phase or at the solid surface by dissociative adsorption

$$O_2(g) \underset{k_{32}}{\overset{k_{31}}{\rightleftarrows}} 2O(g/s) \tag{7}$$

Step 4: oxidation of sulfite ions to sulfate ions

$$\left[SO_3^{2-}\right](s) + O(g/s) \xrightarrow{k_{41}} \left[SO_4^{2-}\right](s) \tag{8}$$

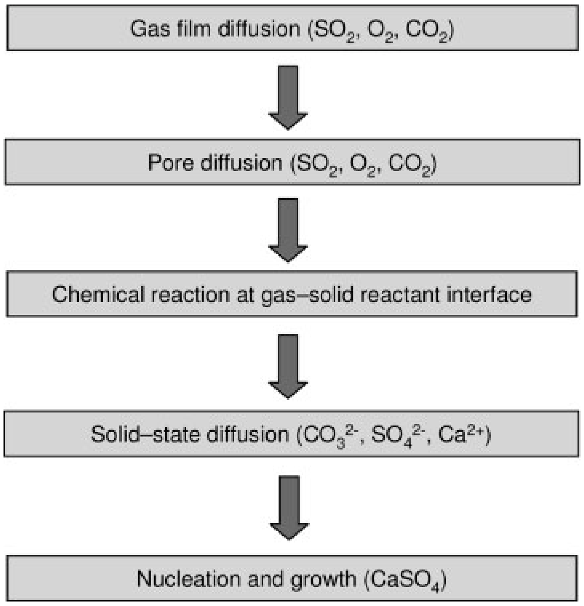

Figure 12. General sequential steps involved in the direct sulfation of limestone.

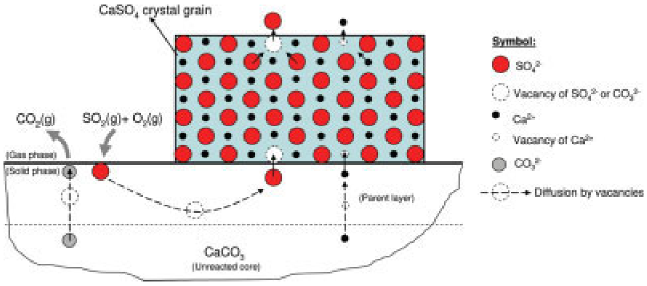

Figure 13. Probable solid-state diffusion process for the nucleation-growth process involved in the direct sulfation of limestone.

[Color figure can be viewed in the online issue, which is available at www.interscience.wiley.com.]

Step 5: desorption of CO_2

$$\cdot[CO_2]_v(s) \underset{k_{52}}{\overset{k_{51}}{\rightleftarrows}} CO_2(g) + [\,]_v(s) \tag{9}$$

For the mechanism suggested above the following assumptions and considerations are made:

Adsorption of SO_2. It was observed that oxidation of SO_2 in the gas phase at the highest-temperature (973 K) applied in the experiments is unnoticeably small without the presence of limestone particles, even though thermodynamically the conversion of SO_2 to SO_3 in the gas phase is favored at such temperatures.[24] This reveals that during the sulfation reaction the oxidation of SO_2 takes place after it is adsorbed on the limestone.

Vacancies of missing carbonate ions in the crystal lattice of calcite at the surface of the parent layer are assumed to be active sites for the adsorption of SO_2. The presence of vacancies in ionic crystalline materials is known to be one of the basic conditions for solid-state diffusion.[22] The space of a vacancy is normally larger than the space that is occupied by a carbonate ion, because of the loss of attraction from negative charges. At the surface of the parent layer, the size of vacancies of carbonate ions is expected to be even larger due to the unsaturated nature of the cations (that is, Ca^2). Vacancies at the surface are probably active sites for the adsorption of SO_2, based on considerations of the size of the vacancy, the probable benefit for lattice energy by the adsorption and especially the dependency of the subsequent diffusion of the formed anions on the vacancies.

Formation of Sulfite. During the process of oxidation of SO_2 to sulfate (SO_4^{2-}), sulfite (SO_3^{2-}) (not $CaSO_3$ in a separate phase) is most likely first formed as an intermediate based on the following observations:

- The absorption of SO_2 on the limestone was observed in this study to proceed in the absence of oxygen.
- Investigation of the intrinsic kinetics of the direct sulfation of limestone showed that the conversion rate of limestone was not affected by variations in O_2 concentration (details of this investigation are reported in a separate article).
- Tullin et al.[13] detected the presence of trace amount of sulfite in the sulfated samples by Fourier transform infrared spectroscopy (FTIR).

The formed sulfite ions are considered to be distributed in the crystal lattice of calcite and do not exist in a separate phase as crystalline calcium sulfite ($CaSO_3$). Crystalline calcium sulfite is likely to form if the sulfite ion concentration reaches the critical level, which, however, will usually not happen with sufficient oxygen in the gas.

Formation of Oxygen Radicals. The sulfite ions are oxidized by the oxidant: oxygen radicals (O) or oxygen in other forms. In this study, there is no clear evidence concerning the form in which oxygen participates in the reaction. Oxygen radicals may come from thermal dissociation of oxygen in the gas phase. Oxygen radicals or oxygen in other forms may also form from dissociative adsorption of oxygen at solid surfaces.[25,26,27,28] In the mechanism suggested earlier, the oxidant is assumed to be oxygen radicals formed by thermal dissociation in the gas phase, and/or by dissociative adsorption at the solid surface.

Formation of Sulfate. As with the formation of sulfite, sulfate ions formed initially are most likely distributed in the crystal lattice of calcite. Calcium sulfate in a separate phase ($CaSO_4$) is first formed when it is nucleated.

Porosity in the product layer

The product layer formed during the direct sulfation reaction has been shown to be porous.[3,4] Snow et al.[2] proposed that the porosity was a result of outflow of CO_2 formed by the sulfation reaction, partly based on the observation of a dense product layer produced during the indirect sulfation reaction (sulfation reaction between SO_2 and calcined limestone), in which CO_2 is not formed. However, our observations indicate that the porosity in the product layer results from the formation of crystal grains of the solid product as shown in Figures 8–10 and illustrated in Figure 11. Porosity in the product layer reflects the presence of free spaces and voids between crystal grains of the solid product, which are clearly visible in Figure 8d. The formation of CO_2 seems therefore to be irrelevant in the development of porosity in the product layer.

The nonrelevance of CO_2 formation to porosity in the product layer is also evidenced by the observations of Duo et al.[29] on the sulfation of calcined limestone (indirect sulfation reaction). The dense product layer formed during the indirect sulfation reaction was believed to reflect the absence of gas (CO_2) evolution during the reaction. However, Duo et al.[29] showed that the product layer produced by the sulfation of calcined limestone can also be porous when the calcined limestone is sintered at high temperatures to form larger dense particles. This fact again demonstrates that the formation of CO_2 during the sulfation reaction is not relevant to porosity in the product layer. In fact, the critical factor seems to be size: the sizes of grains and pores. The product layer formed during the sulfation of calcined limestone is usually dense because the calcined limestone particles typically consist of micrograins of a size around 0.2 μm. The size of micropores between the micrograins is typically around 0.1 μm.[12,14–17,29] The combination of the small sizes of micropores and micrograins makes the pore blocking byproduct crystal grains very easy. Sintering/coalescing of the product crystal grains readily takes place as they are so close together.

Porosity in the product layer can be influenced by various factors, such as conversion, limestone morphology, temperature, and gas composition. With increasing conversion, the free spaces and voids between product crystal grains decrease due to growth of grains and probably coalescence as well. This process explains the observations of decreasing porosity and pore size with increasing conversion.[3,4] The product layer is expected to be more porous for limestones that consist of small calcite grains like Faxe Bryozo, because the random orientation of calcite grains also causes a random orientation of the product crystal grains, which in turn creates more voids. The influence of temperature can be twofold. Temperature has a significant influence on the nucleation process. Porosity and pore size generally increase with increasing temperature due to the formation of fewer, but larger nuclei/crystal grains at higher temperatures.[29] However, at sufficiently high temperatures, sintering of the product crystal grains can become significant, which can cause a decrease in porosity and/or pore size.

Variation in the apparent reaction orders of SO_2, O_2, and CO_2

As observed in this and earlier studies,[1] the apparent reaction order of SO_2 varies with reaction conditions and is significantly lower than unity; O_2 and CO_2 may or may not show influence depending on the reaction conditions. The observations of the influence of these gases were generally made in the second stage of the sulfation where nucleation and crystal grain growth of the solid product were started. The measured sulfation/conversion rate was thus inevitably influenced by the nucleation-growth process, which in conjunction with the resistance of solid-state diffusion and the nature of gas-solid reactions are most likely the reasons for the varying influences of these gases under different reaction conditions. The direct consequence of the occurrence of nucleation and crystal grain growth of the solid product is the reduction of the surface area that is directly available for the sulfation reaction. The conversion rate measured at any given time is partly determined by the fraction of the uncovered surface area of the calcite grains. The apparent reaction order may thus vary significantly depending on the temperature and the conversion.

The presence of significant resistance of solid-state diffusion causes a significant deviation of the calcite surface from the pure state, and, thus, also a slower sulfation rate at the uncovered calcite surface than at pure calcite surface, because of the lowered carbonate activity $a_{CO_3^{2-}}$. The influence of the gaseous reactants is expected to decrease with increasing solid-state diffusion resistance. The resistance of solid-state diffusion is expected to be more significant at lower temperatures, because of its generally high-activation energy, usually significantly higher than 100 kJ/mol. A relevant example is the activation energy for the self diffusion of carbonate ions in calcite lattice which was measured by Haul and Stein[30] to be about 243 kJ/mol. The much lower apparent reaction order of SO_2 measured in this study than in others[5,6,7,8] may partly due to a more significant influence of solid-state diffusion at the relatively low temperatures used in this study.

According to the above suggested reaction mechanism, the sulfation rate is determined by Steps 1, 2 and 5, while Steps 3 and 4 are only steps which convert sulfite ions into the final product: sulfate ions. The rate expressions for Steps 1, 2 and 5 can be established as follows

$$\text{Step 1}: r_1 = k_{11} C_{SO_2} \theta_v - k_{12} \theta_{SO_2} \tag{10}$$

$$\text{Step 2}: r_2 = k_{21} \theta_{SO_2} a_{CO_3^{2-}} \tag{11}$$

$$\text{Step 5}: r_5 = k_{51} \theta_{CO_2} - k_{52} \theta_v C_{CO_2} \tag{12}$$

Here

$$\theta_v + \theta_{SO_2} + \theta_{CO_2} = 1;$$

By assuming that Steps 1 and 5 are in equilibrium, Eq. 11 can be rewritten as follows

$$r_2 = \frac{k_{21} K_1 C_{SO_2} a_{CO_3^{2-}}}{1 + K_5^{-1} C_{CO_2} + K_1 C_{SO_2}} \tag{13}$$

r_2 represents the sulfation rate at the uncovered calcite surface. In Eqs. 11 and 13, $a_{CO_3^{2-}}$ (carbonate activity at the uncovered calcite surface) is a parameter that reflects the influence of solid-state diffusion. $a_{CO_3^{2-}}$ is expected to decrease before the initiation of the nucleation process. Once the nucleation process has begun $a_{CO_3^{2-}}$ at the uncovered calcite surface will not decrease further because the nucleation-growth process acts as a buffer that prevents any further decrease in $a_{CO_3^{2-}}$. With the growth of the product grains, $a_{CO_3^{2-}}$ at the uncovered calcite surface is expected to increase because of the reduced diffusion distance of sulfate ions from the uncovered calcite surface to product grains. Variations in $a_{CO_3^{2-}}$ at the uncovered calcite surface are believed to be one of the main reasons for the variation of the apparent reaction orders of SO_2, O_2 and CO_2 with reaction conditions.

An increase in SO_2 concentration results an increase in the sulfation rate, which in turn causes a decrease in $a_{CO_3^{2-}}$ at the uncovered calcite surface because of the resistance of solid-state diffusion. The apparent observation is thus a reaction order of SO_2 lower than unity which varies with reaction conditions.

The effect of O_2, according to the suggested mechanism, is due to its influence on the concentration of sulfite ions at the uncovered calcite surface. Because of the nucleation and growth process, sulfate ions diffuse immediately away after they are formed, whereas sulfite ions stay. A higher sulfite ion concentration at the uncovered calcite surface means a lower carbonate activity, and, thus, also a lower sulfation rate. The increase in sulfation rate with increasing O_2 concentration is thus caused by the increase in carbonate activity. O_2 shows zero-order behavior when sulfite concentration approaches to zero.

CO_2 has significant influence on solid-state diffusion in calcite[31,32] most likely because of its influence on the formation of extrinsic carbonate vacancies in the crystal lattice of calcite. With increasing CO_2 partial pressure the number of extrinsic carbonate vacancies in the crystal lattice of calcite is reduced, which in turn causes a corresponding decrease in solid-state diffusivity. $a_{CO_3^{2-}}$ at the uncovered calcite surface are thus expected to decrease with increasing CO_2 concentration, and consequently the sulfation rate as well. The influence of CO_2 was observed to become limited at high temperatures,[2,9,33] which may in part be explained by the fact that with increasing temperature the number of extrinsic point defects usually gets less significant compared to the number of intrinsic point defects.[22]

Compared to the established theory, an important feature in the above rate equations is the introduction of the surface activity of carbonate into the rate expressions. This enables consideration of the influence of solid-state diffusion on the sulfation reaction, and provides the necessary bridge between the reaction kinetics and solid-state diffusion for the purpose of modeling.

Controlling mechanism

A reaction process is considered to be controlled by a certain step when that step is so slow that any increase in the rate of other steps that are in series does not result in any significant increase in the overall reaction rate. As discussed earlier, the direct sulfation of limestone involves five general steps, that is, gas-film diffusion, pore diffusion in the particle and product layer, chemical reaction, solid-state diffusion, and the nucleation-growth process. The sulfation process may thus be controlled by each of these steps or by a combination of these steps.

Under the conditions in this study—relatively low-temperatures and very low-conversions, the sulfation process is most likely under mixed control by chemical reaction and solid-state diffusion. Calculations and the measured apparent activation energies indicate that resistances of gas-film diffusion and pore diffusion are negligible. The mixed control by both solid-state diffusion and chemical reaction is practically "guaranteed" by the nucleation-growth process. The resistance of solid-state diffusion is clearly significant in the experiments performed in this study judged by the observed nucleation of the solid product (anhydrite) at relatively low-conversions (for example < 0.5 % at 873 K) in this study. Otherwise, the calcite grain would be sulfated in a pseudo-homogeneous way, as the diffusion of the formed sulfate ions into the inner part of the calcite grain would be fast if solid-state diffusion resistance was insignificant; the conversion rate would also be more or less constant at low-conversions. This is obviously not the case. However, control by solid-state diffusion alone may never be realized because nucleation of the solid product will be initiated before the carbonate activity $a_{CO_3^{2-}}$ at the uncovered surface of the calcite grain drops to zero due to thermodynamic reasons. Chemical reaction can influence the sulfation reaction as long as the carbonate activity $a_{CO_3^{2-}}$ at the uncovered surface of the calcite grain doesn't drop to zero. The significant influence of chemical reaction rate is reflected by the significant effect of SO_2 and O_2 on the overall sulfation rate.

Influence of water

As shown earlier, water promoted the direct sulfation of limestone. A probable explanation of the effect of water is its influence on solid-state diffusion by the formation of hydroxide ions (OH^-). The movement of cations (Ca^2) is an important part of the nucleation-growth process and may contribute a significant part of the resistance of solid-state diffusion. The formation of hydroxide ions and their adsorption in anion sites (carbonate)[34,35] in the crystal lattice of calcite may result in the formation of more cation (Ca^2) vacancies, as hydroxide ions are of single valence. The increase of the number of cation vacancies improves the diffusion of the cations and thus solid-state diffusion in general.

Addition of water to the gas in this and earlier studies[5] was observed to increase the apparent reaction orders of SO_2 and O_2. This phenomenon seems to be in agreement with water's probable improvement on solid-state diffusion. Direct sulfation of limestone is usually under mixed control by both chemical reaction and solid-state diffusion. An improvement on solid-state diffusion makes the chemical reaction more dominant in the mixed control. The increase in the apparent reaction orders of SO_2 is probably a reflection of the increased control by chemical reaction.

Modeling

The shrinking unreacted core model[18,23] is frequently used to model the direct sulfation of limestone.[1] Generally, the concept of shrinking unreacted core is considered applicable for the direct sulfation of limestone. However, the simplified shrinking unreacted core model that are described in Levenspiel[18] and Szekely et al.[23] are insufficient for the direct sulfation of limestone; this is because these models do not consider factors such as:

- The direct sulfation of limestone involves the nucleation-growth process.
- The direct sulfation of limestone is significantly influenced by solid-state diffusion.
- Reduction in the directly available surface area for the sulfation reaction is caused by both shrinking of the unreacted core and the formation of product crystals. The directly available surface area for the sulfation reaction, is, therefore, expected to be significantly smaller than the total surface area of the unreacted core.
- The properties of the product layer (such as porosity and pore size) vary during the sulfation process due to crystal grain growth of the solid product and sintering.

Model simulations are often used for the extraction of kinetic parameters, and for the judgment of controlling mechanisms. The use of the simplified shrinking unreacted core model for the modeling of the direct sulfation of limestone without considering these aspects may lead to erroneous results and conclusions. For example, the effective diffusivity in the product layer was often evaluated across the whole thickness of the product layer. However, considering (1) that the resistance of solid-state diffusion is most likely the major diffusion resistance, and (2) that this resistance of solid-state diffusion is probably located at the surface of the unreacted core at low conversions, and in a relatively thin layer near the unreacted core at high conversions, the effective diffusivity evaluated in such a way is no more than a model parameter and does not represent any physical properties of diffusion in the gas phase or in the solid phase.

Conclusions

The direct sulfation of limestone involves oriented nucleation and crystal grain growth of anhydrite-the only final solid product. Five general steps can be defined for the direct sulfation of limestone. They are gas film diffusion, pore diffusion, chemical reaction, solid-state diffusion and the nucleation and crystal grain growth of the solid product.

The direct sulfation of limestone can be significantly influenced by the concentrations of the gaseous reactants (SO_2 and O_2) and gaseous product (CO_2), and the presence of water as well. The strength of the influences of these gases varies with reaction conditions. At 823 K, and in the absence of water, the influence of SO_2, O_2 and CO_2 on the direct sulfation of limestone corresponds to apparent reaction orders of approximately 0.2, 0.2 and −0.5, respectively. The presence of water in the gas phase significantly increases the sulfation rate and the apparent reaction orders of SO_2 and O_2. At high O_2 concentrations ($>$ approximately 15 %), the apparent reaction order of O_2 drops to zero.

At low temperatures and low conversions, the direct sulfation reaction is usually under mixed control by chemical reaction and solid-state diffusion partly because of the interaction of the nucleation-growth process. The low apparent reaction orders of SO_2 and O_2, their variations with the reaction conditions, and the influence of water are closely related to the controlling mechanism, and the effect of reaction conditions on solid-state diffusion and the nucleation-growth process.

Carbonate activity at calcite surface, a new parameter is introduced in this article for describing kinetic behaviors of the direct sulfation of limestone. This new parameter represents the influence of solid-state diffusion in the sulfation process and reflects as well the true situation at the gas-solid reactant interface.

The chemical reaction that takes place at the surface of the gas-solid reactant interface may involve steps, such as the adsorption of SO_2 in active sites at the surface of the solid reactant, the formation of sulfite ions (SO_3^{2-}) as an intermediate, further oxidation of the formed sulfite ions to form sulfate ions, and desorption of CO_2. The effect of O_2 is most likely due to its influence on the concentration of sulfite ions at calcite surface.

The product layer formed during the direct sulfation of limestone is a collection of crystal grains of the solid product ($CaSO_4$). The presence of spaces and voids between the crystal grains is the reason for porosity in the product layer. The decrease in porosity and pore size with increasing conversion is due to the reduction in these spaces and voids caused by growth of the crystal grains of the solid product, and probably also sintering.

In the aspect of kinetic modeling, the finding of this study—the nucleation and crystal grain growth of the solid product and its importance— indicates that the simplified shrinking unreacted core model (which considers only the resistances of gas film diffusion, pore/product-layer diffusion and chemical reaction) is inadequate to describe the direct sulfation of limestone, if it, in addition to the purpose of process simulation, is used as well for the assessment of reaction mechanism and extraction of kinetic parameters, such as intrinsic rate constants and solid-state diffusivity. For avoiding the shortcomings of the simplified shrinking unreacted core model, new models for the modeling of the direct sulfation of limestone at relatively low temperatures and low conversions are developed and presented in a separate article.

Acknowledgments

This work is part of the CHEC (Combustion and Harmful Emission Control) Research Center funded a.o. by the Technical University of Denmark, the Danish Technical Research Council, the European Union, the Nordic Energy Research, Dong Energy A/S, Vattenfall A.B., F L Smidth A/S, and Public Service Obligation funds from Energinet.dk and the Danish Energy Research program. This particular work is financially supported by the Technical University of Denmark and FLSmidth A/S. We would like to thank Mr. Ole Johnsen of the Geological Museum, University of Copenhagen, Denmark, for supplying the sample of Iceland Spar for the experiments.

Notation

a = solid-state activity
C = concentration
E_a = activation energy
K = equilibrium constant
k = reaction rate constant
M_{CaCO_3} = molar weight of $CaCO_3$
P = total pressure
p = partial pressure
R = gas constant
r = surface reaction rate
t = time
T = temperature
V = gas flow
W = bed weight
x = conversion of solid reactant (limestone)
y = molar fraction
ζ = fraction of $CaCO_3$ in limestone
θ_v = fraction of vacant active sites for the adsorption of SO_2 and CO_2
θ_{SO_2} = fraction of active sites occupied by SO_2
θ_{CO_2} = fraction of active sites occupied by CO_2
$[\ ]_v$ = vacant active site
$[SO_2]$ = active site occupied by SO_2
$[CO_2]$ = active site occupied by CO_2
$[SO_3^{2-}]$ = carbonate site occupied by a sulfite ion
$[SO_4^{2-}]$ = carbonate site occupied by a sulfate ion

Subscript

av = average

Literature Cited

1. Hu G., Dam-Johansen K, Wedel S, Hansen JP. Review of the direct sulfation reaction of limestone. *Progr in Energy and Comb Sci.* 2006;32:386–407.
2. Snow MJH, Longwell JP, Sarofim AF. Direct sulfation of calcium carbonate. *Ind Eng Chem Res.* 1988;27:268–273.
3. Hajaligol MR, Longwell JP, Sarofim AF. Analysis and Modeling of the direct sulfation of $CaCO_3$. *Ind Eng Chem Res.* 1988;27:2203–2210.
4. Liu H, Katagiri S, Kaneko U, Okazaki K. Sulfation behaviour of limestone under high CO_2 concentration in O_2/CO_2 coal combustion. *Fuel.* 2000;79:945–953.
5. Yang RT, Cunningham PT, Wilson WI, Johnson SA. Kinetics of the reaction of half-calcined dolomite with sulfur dioxide. *Adv Chem Ser.* 1975. *Sulfur Removal Recovery Ind. Processes, Symp.* 1974; 139:149–157.
6. Iisa K, Hupa M and Yrjas P. Product layer diffusion in the sulfation of calcium carbonate. *Twenty-Fourth International Symposium on Combustion The Combustion Institute.* Sydney, Australia 1992;1349–1356.
7. Krishnan SV, Sotirchos SV. Sulfation of high purity limestones under simulated PFBC conditions. *Can J Chem Eng.* 1993;71:244–255.
8. Qiu K, Lindqvist O. Direct sulfation of limestone at elevated pressures. *Chem Eng Sci.* 2000;55:3091–3100.
9. Iisa K and Hupa M. Sulfur absorption by limestone at pressurized fluidized bed conditions. *Twenty-Third International Symposium on*

Combustion The Combustion Institute. 1990;943–948.

10. Alvarez E, Gonzalez JF. High pressure thermogravimetric analysis of the direct sulfation of Spanish calcium-based sorbents. *Fuel*. 1999;78:341–348.
11. Ulerich NH, Newby RA and Keairns DL. A thermogravimetric study of the sulfation of limestone and dolomite-prediction of pressurized and atmospheric fluidized-bed desulfurization. *Thermochim Acta*. 1980;36:1–16.
12. Dam-Johansen K. *Absorption of SO_2 on Dry Limestones*. (in Danish) Department of Chemical Engineering, Denmark Technical University; 1987. Ph.D. thesis.
13. Tullin C, Nyman G and Ghardashkhani S. Direct Sulfation of $CaCO_3$: The influence of CO_2 partial pressure. *Energy & Fuels*. 1993;7:512–519.
14. Dam-Johansen K, Østergaard K. High-temperature reaction between sulfur dioxide and limestone-I. Comparison of limestone in two laboratory reactors and a pilot plant. *Chem Eng Sci*. 1991;46(3):827–837.
15. Dam-Johansen K, Østergaard K. High-temperature reaction between sulfur dioxide and limestone-II. An improved experimental basis for a mathematical model. *Chem Eng Sci*. 1991b;46(3):839–845.
16. Dam-Johansen K, Hansen PFB, Østergaard K. High-temperature reaction between sulfur dioxide and limestone-III. A grain-micrograin model and its verification. *Chem Eng Sci*. 1991c;46(3)847–853.
17. Dam-Johansen K, Østergaard K. High-temperature reaction between sulfur dioxide and limestone-IV. *Chem Eng Sci*. 1991d;46(3):855–859.
18. Levenspiel O. *Chemical Reaction Engineering*. New York: John Wiley and Sons, Inc., 1999.
19. Fuertes AB, Velasco G., Fuente E, Parra JB, Alvarez T. Sulfur retention by limestone particles under PFBC conditions. *Fuel Process Technol*. 1993;36:65–71.
20. Murthy KS, Howes JE, Nack H. Emissions from pressurized fluidized-bed combustion processes. *Am Chem Soc*. 1979;13(2):197–204.
21. Ljungström E, Lindqvist O. Measurement of in-bed gas and solid compositions in a combustor operating at pressures up to 20 bar. *7th International Conference on Fluidized Bed Combustion*. Philadelphia, PA; 1982;465–472.
22. West AR. *Basic Solid State Chemistry*. Chichester: John Wiley; 1999.
23. Szekely J, Evans JW, Sohn HY. *Gas-Solid Reactions*. New York: Academic Press; 1976.
24. Schenk PW, Steudel R.Chapter 11. In: *Nickless G. Inorganic Sulfur Chemistry*.Elsevier Publishing Co., Ltd; 1968.
25. Roberts MW, Smart RSC. Evidence from photoelectron spectroscopy for dissociative adsorption of oxygen on nickel oxide. *Surface Sci*. 1981;108:271–280.
26. Henrich VE. Fundamentals of gas-surface interactions on metal oxides. *Appl Surface Sci*. 1993;72:277–284.
27. Cordero F, Cantelli R. Interstitial O and O vacancies in $La_2CuO_{4+\delta}$ during high-temperature treatments. *Physica C*. 1999;312:312–224.
28. Palmer MS and Neurock MJ. Periodic density functional theory study of the dissociative adsorption of molecular oxygen over La_2O_3. *Phys Chem B*. 2002;106:6543–6547.
29. Duo W, Laursen K, Lim J, Grace J. Crystallization and fracture: formation of product layers in sulfation of calcined limestone. *Powder Technol*. 2000;111:154–167.
30. Haul, RAW, Stein LH. Diffusion in calcite crystals on the basis of isotopic exchange with carbon dioxide. *Trans of the Faraday Soc*. 1955;51:1280–1290.
31. Beruto D, Giordani M, Botter R. Microstructure development of Li_2CO_3-$CaCO_3$ eutectic mixture in CO_2 (g) and N_2 (g) environment. *J Physique, Colloque C1, Supplement au n°2*. 1986;47:C1-527–531.
32. Tetard F, Bernache-Assollant D, Champion E. Pre-eutectic densification of calcium carbonate doped with lithium carbonate. *J Therm Anal Calorimetry*. 1999;56:1461–1473.
33. Illerup JB, Dam-Johansen K and Lunden K. High-temperature reaction between sulfur dioxide and limestone-VI. The influence of high pressure. *Chem Eng Sci*. 1993;48(11):2151–2157.
34. Eastman PF and Cutler IB. Effect of water vapor on initial sintering of magnesia. *J Am Cera Soc*. 1966;49(10):526–530.
35. Razouk RI, Mikhail RS, Ragai J. Surface properties of calcined magnesia: effects of presence of water vapor on surface areas and pore sizes. *J Appl Chem Biotechnol*. 1973;23:51–61.

Manuscript received May 9, 2006, and revision received Jan. 9, 2007.